Check for updates

Contrasting Impacts of Climate Warming on Coastal Old-Growth Tree Species Reveal an Early Warning of Forest Decline

Catherine Mercer[1]*, Vanessa M. Comeau[2], Lori D. Daniels[2] and Marco Carrer[3]

[1] Department of Biological and Environmental Sciences, University of Stirling, Stirling, United Kingdom, [2] Department of Forest and Conservation Sciences, University of British Columbia, Vancouver, BC, Canada, [3] Department Territorio e Sistemi Agro-Forestali, Università di Padova, Padua, Italy

Old-growth forests in the Pacific Northwest are being fundamentally altered by climate change. A primary example of this is yellow-cedar (*Callitropsis nootkatensis*), a culturally and economically important species, which has suffered widespread decline across its range since the beginning of the twentieth century. We used tree rings to compare the climate-growth response of yellow-cedar to two co-occurring species; western hemlock (*Tsuga heterophylla*) and Sitka spruce (*Picea sitchensis*), in an old-growth forest on Haida Gwaii, Canada, to better understand the unique climatic drivers of a species that is declining across its range. We developed three species-specific chronologies spanning 560–770 years, reconstructing a long-term record of species growth and dynamics over time. The climate is strongly influenced by the Pacific Decadal Oscillation (PDO), a multi-decadal pattern of ocean-atmospheric climate variability. Climate varied across three time periods that have coincided with major shifts in the PDO during the twentieth century [1901–1945 (neutral/positive), 1946–1976 (negative) and 1977–2015 (positive)]. Conditions were significantly warmer and wetter during positive phases, with the greatest maximum temperatures in the most recent period. We used complimentary methods of comparison, including Morlet wavelet analysis, Pearson correlations, and linear-mixed effects modeling to investigate the relations between climate and species growth. All three species exhibited multi-decadal frequency variation, strongest for yellow-cedar, suggesting the influence of the PDO. Consistent with this, the strength and direction of climate-growth correlations varied among PDO phases. Growing season temperature in the year of ring formation was strongly positively correlated to yellow-cedar and western hemlock growth, most significantly in the latter two time periods, representing a release from a temperature limitation. Sitka spruce growth was only weakly associated with climate. Yellow-cedar responded negatively to winter temperature from 1977 to 2015, consistent with the

decline mechanism. Increased yellow-cedar mortality has been linked to warmer winters and snow loss. This study provides new insights into yellow-cedar decline, finding the first evidence of decline-related growth patterns in an apparently healthy, productive coastal temperate rainforest.

INTRODUCTION

Forest ecosystems are becoming increasingly impacted by warming associated with climate change (Adams et al., 2009; van Mantgem et al., 2009; Allen et al., 2010). Adaptation to and mitigation of these effects will depend on an increased understanding of how forests respond, which is highly location- and species-specific (e.g., Holman and Peterson, 2006). At high elevation and high latitude, increased growing season temperature and length as the regional climate warms (Cayan et al., 2001; Christidis et al., 2007) will likely facilitate increased tree growth (Nemani et al., 2003). For example, enhanced tree growth has been documented across the boreal forest, where trees are experiencing a "greening" response to increased temperature (Driscoll et al., 2005; Wilmking and Juday, 2005; Lloyd et al., 2011). However, warmer drier conditions can also be detrimental (Allen et al., 2010). Research on divergence in tree-ring widths has revealed that for many species warm temperatures eventually become limiting, due to direct temperature stress or moisture stress (D'Arrigo et al., 2004; Wilmking et al., 2004; Driscoll et al., 2005; Lloyd and Bunn, 2007). As the climate continues to warm, the interaction between temperature and moisture plays a critical role. Non-growing season climate and interactions with extreme events can also drive change. Warming winter temperatures, are leading to reduced snowpack levels (Groisman et al., 2004; Knowles et al., 2006), with consequences for water supply from spring snowmelt runoff (Stewart et al., 2004) and species that rely on persistent snow cover in late-winter as protection from thaw-freeze events (Buma et al., 2019). Species sensitive to winter climate include yellow-cedar [*Callitropsis nootkatensis* (D. Don) D.P. Little] along the Pacific coast of British Columbia (BC), Canada and Alaska, United States (Schaberg et al., 2008; Hennon et al., 2012) and yellow birch (*Betula alleghaniensis*) in eastern forests of North America (Bourque et al., 2005). Predicting the response of forests to climate is highly species-specific, as tree species have unique environmental adaptions and competitive strategies (Lévesque et al., 2013; Meyer et al., 2020), and within a species there can be divergence in climate-growth responses through time (D'Arrigo et al., 2008).

High-latitude coastal temperate rainforests are a unique case, as they are thought to be radiation- and temperature-limited (Boisvenue and Running, 2006) and, therefore, likely to benefit from increasing temperature with little concern for moisture availability. Because coastal climates are moderated by the proximity to the ocean, variation in the growth of coastal trees is low from year to year, with stronger correlations to decadal variations in nearby ocean basins (Gedalof and Smith, 2001; Tucker and Pearl, 2021). In general, the vulnerability of this forest ecoregion to climate change is considered very low to medium (Wang et al., 2019). However, across coastal temperate rainforests globally, warming temperatures are crossing key climatic and ecological thresholds (Veblen et al., 2011; Shanley et al., 2015). Along the Pacific coast of North America, average annual temperatures range from 4 to 12°C (DellaSala, 2011), and importantly winter temperatures exist near the rain-to-snow threshold (−2 to 2°C) (Buma et al., 2019). Therefore, although changes in temperature in coastal regions have not been as extreme as other high-latitude regions, small changes in temperature have had significant impacts (Buma, 2018; Buma et al., 2019).

Old-growth temperate rainforests at high latitudes along the Pacific coast of North America are often co-dominated by yellow-cedar, Sitka spruce (*Picea sitchensis* Bong.) and western hemlock [*Tsuga heterophylla* (Raf.) Sarg.] All three species are long-lived conifers that coexist in old-growth forests through subtle differences in regeneration dynamics in canopy gaps created by fine-scale disturbances (Harris, 1990; Taylor, 1990; Lertzman et al., 1996) and differential longevity (Lertzman, 1995). Of the three species, yellow-cedar lives longest with maximum lifespans exceeding 1,000 years, so that low abundance of regeneration and infrequent recruitment in canopy gaps is sufficient to sustain populations (Lertzman, 1992). Sitka spruce is least shade-tolerant, commonly regenerates following stand-level disturbance and grows rapidly. In late-successional forests it depends on relatively large canopy gaps to regenerate, requiring a few large gaps over several decades for trees to recruit and persist as a co-dominant in the canopy (Harris, 1990; Taylor, 1990). Western hemlock is very shade-tolerant and highly responsive to gaps, with the smallest and slowest growing individuals exhibiting the greatest growth release following gap formation (Packee, 1990; Stan and Daniels, 2010). Dense seedlings and saplings persist in the understory for decades to centuries waiting to exploit a gap and recruit to the canopy (Stan and Daniels, 2010); however, western hemlock seedling and sapling survival, growth rates, and average tree lifespans are lower than Sitka spruce or yellow-cedar (Taylor, 1990; Lertzman, 1992).

Although yellow-cedar, western hemlock and Sitka spruce have coexisted in old-growth forests for millennia (Hennon et al., 2016), they also exemplify the species-specific nature of climate impacts on tree growth and survival. Yellow-cedar is an example of the positive and negative effects of anthropogenic climate change (Beier et al., 2008; Comeau et al., 2019). Warm growing season temperatures facilitate growth of healthy yellow-cedars (Laroque and Smith, 1999; Beier et al., 2008; Comeau et al., 2019). Yet, yellow-cedar is undergoing widespread crown dieback and tree mortality in approximately 400,000 ha of its

range (Hennon et al., 2005; Buma et al., 2017). Tree dieback and death have been linked to fine-root damage by late-winter thaw-freeze events, which drives physiological drought stress during the subsequent growing season (D'Amore and Hennon, 2006). Yellow-cedar roots grow in the upper organic and mineral soil horizons on sites with shallow water tables and the trees take advantage of warm periods in the early spring for nutrient uptake, when co-occurring species remain dormant (Hennon et al., 2016). Early root activity increases susceptibility to frost damage in years of low snowpack, the risk of which has increased over the twentieth century due to warming winter temperatures (D'Amore and Hennon, 2006; Schaberg et al., 2008). Consistent with these mechanisms, research in southeastern Alaska and on Haida Gwaii, BC, has demonstrated that yellow-cedars in declining stands are limited by warm dry winter conditions (Beier et al., 2008; Wiles et al., 2012; Comeau et al., 2019).

Western hemlock and Sitka spruce co-occur with yellow-cedar, but they do not exhibit symptoms of decline and may be more able to take advantage of warming temperatures. For example, growth of western hemlock in Washington (United States) was positively correlated with growing season temperature and annual precipitation, but negatively correlated with consecutive years of high snowfall (Rudnicki and Chen, 2000). The latter is opposite to the association between declining yellow-cedar stands and low winter snowpack. Several phenotypic traits of Sitka spruce have been associated with mean annual temperature and mean coldest month, with precipitation variables explaining less variation than temperature variables (Holliday et al., 2010; Mimura and Aitken, 2010). Thus, it is likely that western hemlock and Sitka spruce growth will benefit from increased growing season temperatures and lengthened growing season at high latitudes (e.g., Nemani et al., 2003), but site-specific research is needed.

Anticipating how these forests will respond to future climate change can be informed by understanding how the component species have responded to past variation in climate at a range of temporal scales. Tree growth along the Pacific coast is strongly influenced by natural climate variability associated with the Pacific Decadal Oscillation (PDO) (D'Arrigo et al., 2001; Gedalof and Smith, 2001). The PDO is characterized by multi-decadal changes in sea-surface temperature that alter the regional climate (Mantua et al., 1997; Mantua and Hare, 2002). In the twentieth century, the PDO is thought to have undergone a regime shift to a negative phase in 1945–1946 and a shift to a positive phase in 1976–1977. Along the northern Pacific coast of North America, negative PDO phases are associated with cooler and drier climate conditions, while positive shifts bring warmer and wetter conditions, including reduced snow depth and earlier snowpack melting (Mantua and Hare, 2002). Thus, comparing climate-growth response between PDO phases can provide insights into species-specific growth sensitivity to warm growing season temperatures and winter thaw-freeze events.

We sampled canopy-dominant yellow-cedar, western hemlock and Sitka spruce in an old-growth forest with no visible symptoms of canopy dieback, located on Haida Gwaii, Canada. Our study is the first to examine yellow-cedar climate-growth dynamics in comparison with co-occurring species. Given the regional influences of the PDO along the north Pacific coast, we compared climate and the climate-growth response of each species across three periods associated with PDO regime shifts in the twentieth century: 1901–1945 (neutral/positive phase), 1946–1976 (negative phase), 1977–2015 (positive phase). Following Mantua and Hare (2002) and Comeau et al. (2019), we expected that the climate would be warmer and wetter in positive phases of the PDO, but cooler and drier in the negative phase. We hypothesized that the growth of all three species would be positively associated with growing season temperatures, particularly during the positive phases of the PDO, as tree species in high latitude forests are commonly temperature-limited. In positive phases, we also hypothesized yellow-cedar growth would be negatively associated with winter temperature and precipitation, given that warmer winter temperature and low snowpack depth has been linked to species decline (Hennon et al., 2012).
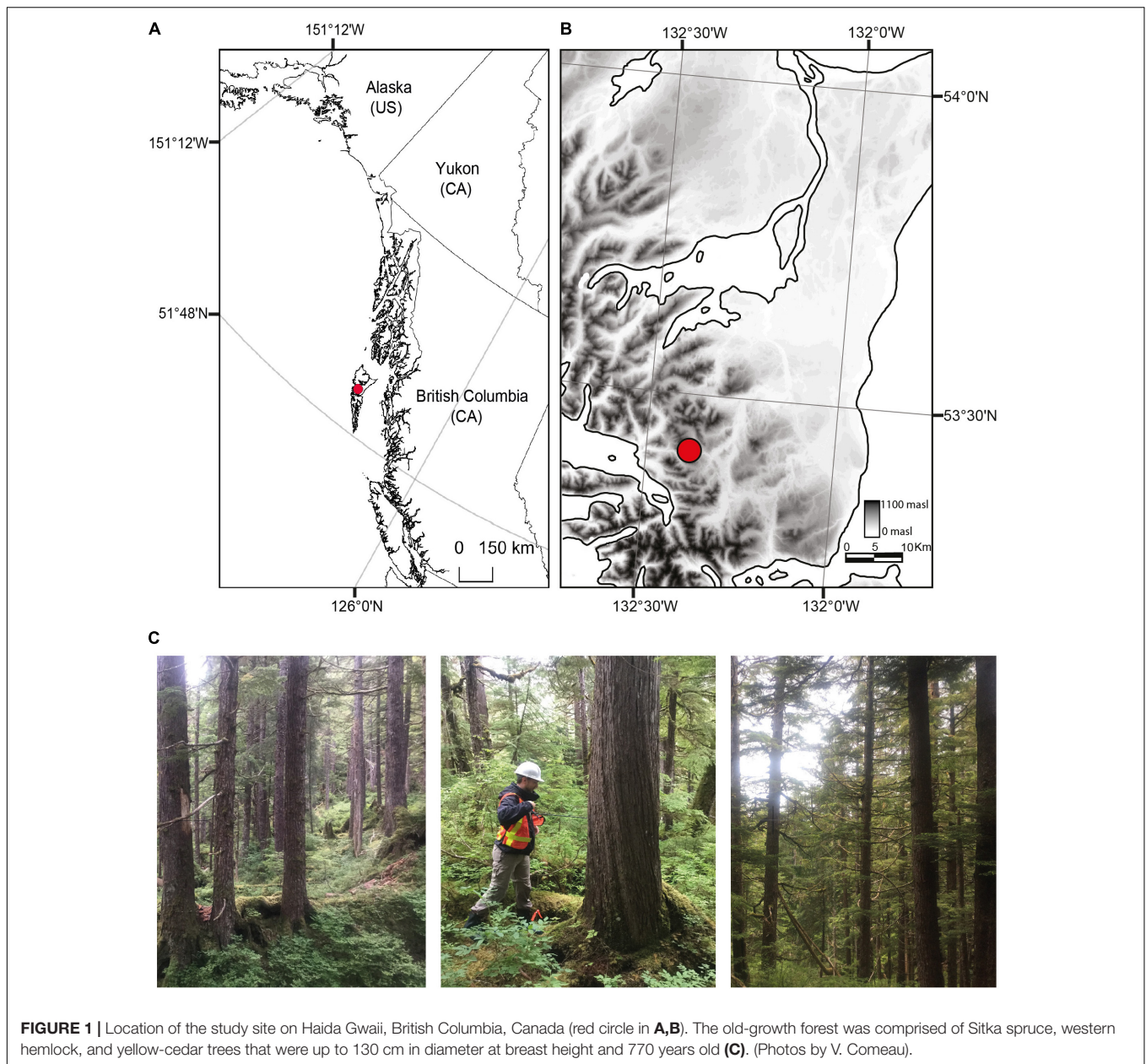
MATERIALS AND METHODS

Study Area

We sampled a mixed-species old-growth forest on Haida Gwaii (53° 23′ 50.97″ N, -132° 22′ 31.52″ W; 394 meters above sea level), located on the Pacific coast of British Columbia, Canada (**Figure 1**). The BC Government Vegetation Resources Inventory (VRI), a landscape wide data layer derived from aerial photo interpretation and ground sampling, indicates there was no evidence that stand-level wind, fire, insects, pathogens, or yellow-cedar decline were driving tree mortality at our study site (BC Government, 2020). The VRI data estimates tree species composition, age, volume and height. The most recent VRI data for our study area indicates that the dominant species were western hemlock (55%) and Sitka spruce (30%), with smaller proportions of yellow-cedar and western redcedar, the average age of canopy trees was > 350 years, average height was 38 m with non-uniform vertical complexity, and basal area was 65 m^2 per hectare (ha) (BC Government, 2020). Density within the VRI polygon was 325 live and 5 dead trees ha^{-1}, with 55% crown closure (BC Government, 2020).

The forest is located in the montane variant of the Wet Hypermaritime Coastal Western Hemlock subzone (CWHwh), according to biogeoclimatic classification (Meidinger and Pojar, 1991). Climate of the stand is classified as warm temperate, humid, with cool summers (Cfc, Kottek et al., 2006). From 1901 to 2015, the stand had an annual average temperature of 6.06°C (±0.68°C) and average total precipitation of 2,292 mm (±276 mm) annually (ClimateBC, Wang et al., 2016).

Field Sampling, Chronology Building, and Assessment

Starting from the center of the forest stand, we searched an expanding area until we sampled 60 canopy trees, 20 each of yellow-cedar, western hemlock and Sitka spruce. Following standard dendroclimatological methods (Fritts, 1976), we selected large (diameter at breast height = ∼50−130 cm) and presumed old, living individuals of each species and one core was

FIGURE 1 | Location of the study site on Haida Gwaii, British Columbia, Canada (red circle in **A,B**). The old-growth forest was comprised of Sitka spruce, western hemlock, and yellow-cedar trees that were up to 130 cm in diameter at breast height and 770 years old **(C)**. (Photos by V. Comeau).

collected from each tree at breast height to generate the longest ring-width series possible.

Cores were air-dried, mounted on wooden supports, and sanded with increasingly finer grains to 600 grit. The cores were scanned at a high resolution (2400 or 3200 dpi) and the CooRecorder program was used to measure the width of rings to the closest 0.001 mm (Larsson, 2014a). Ring-width series were cross-dated using the program CDendro to create species-specific ring-width chronologies (Larsson, 2014b). The program COFECHA was used to confirm cross-dating accuracy (Holmes, 1983). For each species, two detrended chronologies were developed using the dplR package in R (Bunn et al., 2021; R Core Team, 2021), as follows. First, a negative exponential curve was fit to individual tree ring-width series to remove size- and age-related trends, resulting in standard chronologies used for wavelet analysis (below). Second, individual ring-width series were double detrended, fitting a negative-exponential curve to the ring-width series, followed by a 60-year spline (50% frequency response) that removed longer term growth trends. The chosen spline retained > 95% of variance at < 31 years, allowing us to test for the potential influences of multi-decadal variation associated with the PDO. Finally, each double-detrended ring-width series was pre-whitened using an autoregressive model to remove temporal autocorrelation and species residual chronologies were created by averaging across the pre-whitened series (Cook and Holmes, 1996).

Summary statistics derived for each chronology included the length of the chronology, mean sensitivity (MS), a measure

of year-to-year ring-width variability, and the inter-series correlation (rbar), a measure of the correlation among all ring-width series (Fritts, 1976). The expressed population signal (EPS) measured the strength of the common signal among series (Wigley et al., 1984). We averaged the EPS from 1901 to 2015, the period used for climate-growth analysis. Summary statistics were reported for the residual chronologies.

To identify dominant modes of temporal variability, we performed a Morlet wavelet analysis on the standard species-specific chronologies (Torrence and Compo, 1998). Wavelet analysis was conducted across the length of the shortest species chronology, to aid comparison between species. We analyzed wavelengths from 1457 to 2015, the length of the Sitka spruce chronology at the site. The default parameter settings of the Morlet wavelet function in dplR were used, with a 95% confidence interval chosen for estimating the cone of influence (Bunn et al., 2021).

Climate-Growth Analysis

Climate data for the study site were obtained using ClimateBC, a climate mapping software that downscales historical monthly climate variables, from local weather stations and regional climate models, at a spatial resolution of $0.5° \times 0.5°$ (Wang et al., 2016). Historical monthly climate data were obtained for 1901–2015 by inputting the site coordinates into ClimateBC. The full climate record was split into periods, based on well-documented regime shifts in the PDO: 1901–1945 (neutral/positive phase), 1946–1976 (negative phase) and 1977–2015 (positive phase) (Mantua and Hare, 2002). To test if climate varied significantly among PDO phases, we compared monthly temperature (mean, minimum, and maximum) and total precipitation among phases using a Kruskal-Wallis one-way analysis of variance on ranks, with a Dunn's *post-hoc* test ($\alpha = 0.05$ for all statistical tests).

To assess relationships between growth and climate, we correlated the residual chronology of each species against monthly temperature and precipitation data using the treeclim package in R (Zang and Biondi, 2015). In preliminary analyses, we correlated mean, minimum, and maximum monthly temperatures from 1901 to 2015 against the residual chronologies. Significant correlations ($p < 0.05$) were identified using bootstrapped samples ($n = 1,000$). Subsequent analyses used maximum temperature, which was most significantly correlated with growth of all three species. To compare among species, the residual chronologies were correlated against monthly maximum temperature and total precipitation, across the full 1901–2015 record and three periods (1901–1945, 1946–1976, 1977–2015). In each analysis, correlations were calculated for a 15-month window, from June of the year prior to ring formation through August of ring formation to assess potential lagged effects of the previous growing season, fall, or winter climate.

We developed species-specific linear-mixed effects models for each time period to quantify growth response to climate, while accounting for variability in growth among individual trees (hereafter "predictive effect"). This analysis is being increasingly used to understand the key climate drivers of tree growth across time (Carrer et al., 2019). Mixed-model analysis was undertaken

in R using the nlme package (Pinheiro et al., 2021). Each model was structured as:

$$Y_i = \alpha + X_i\beta + b_i + \varepsilon_i$$

where Y_i is a vector of residual ring-width index values for tree i, α is the model intercept, X_i is a matrix of fixed effects (monthly and seasonal climate variables), β is a vector of fixed effects coefficients, b_i is the random effect (ID of tree i) and ε_i represents the error term. Models were fitted with random intercepts, assuming the relationship between climate and growth was constant between conspecific trees. Only residual ring-width index series that spanned the full common time period (1901–2015) were included. A combination of monthly and seasonal climate variables was selected as fixed effects, based on the Pearson correlation analysis and previous studies of yellow-cedar growth on Haida Gwaii (Comeau et al., 2019). Monthly climate variables included maximum temperature of September (pTMAX$_{Sept}$) and November (pTMAX$_{Nov}$) in the year prior to ring formation, and current August precipitation (P$_{Aug}$). Five seasonal climate variables were derived as follows. Previous summer temperature (pTMAX$_{Sum}$) was the average of previous June–August maximum temperatures; winter temperature (TMAX$_{Winter}$) averaged December to February maximum temperatures; spring temperature (TMAX$_{Spring}$) averaged March to May maximum temperatures, and summer temperature (TMAX$_{Sum}$) averaged current June to August maximum temperatures; and winter precipitation (P$_{Winter}$) was the sum of December to February precipitation. We chose a backward model selection approach to determine the climate variables that most explained residual ring-width index growth, by removing the least significant climate variables until all variables in the model were significant. To increase interpretability of the model coefficients, the fixed effects were centered and then scaled to create z-scores. A test of collinearity between fixed effect variables was performed on each full model, with all fixed effects included, by testing the variance inflation factor (VIF). We inspected the model diagnostics to ensure there were no outliers and the residuals were normally distributed with no heteroscedastic variability. We reported the intercept, coefficient estimate, standard error, and p-value for each model. To assess model fit we computed the marginal R^2 (Nakagawa et al., 2017) and root mean square error (RMSE) for each of the nine species and time combinations.

RESULTS

Chronology Variation and Wavelet Analysis

Ring-width series from large and old trees contributed to each species-specific residual chronology, which spanned 559–773 years (**Table 1**). The yellow-cedar chronology included 19 ring-width series that were longer, on average, than those of western hemlock and Sitka spruce. Of the three species, yellow-cedar had the highest inter-series correlations (rbar = 0.482) and inter-annual growth variability (MS = 0.271). Western hemlock

TABLE 1 | Descriptive statistics of full-length species residual chronologies.

Species	N years	M years	N	MRW	SD	rbar	MS	EPS Y/Avg.
Yellow-cedar	1243–2015 (773 years)	472	19	0.69	0.416	0.482	0.271	1776/0.89
Western hemlock	1366–2015 (650 years)	370	14	0.65	0.336	0.314	0.241	0.78
Sitka spruce	1457–2015 (559 years)	298	20	1.10	0.500	0.400	0.217	0.82

N years = length of chronology; M years = mean series length; N = number of series contributing to the chronology; MRW = mean ring-width (mm); SD = ring-width standard deviation (mm); rbar = inter-series correlation; MS = mean sensitivity; EPS Y/Avg. = year when the expressed population signal passed 0.85 (no value indicates that the EPS did not pass and stay above 0.85)/the average EPS from 1901 to 2015. rbar, MS and EPS Y/Avg. were calculated using the residual ring-width index chronologies.
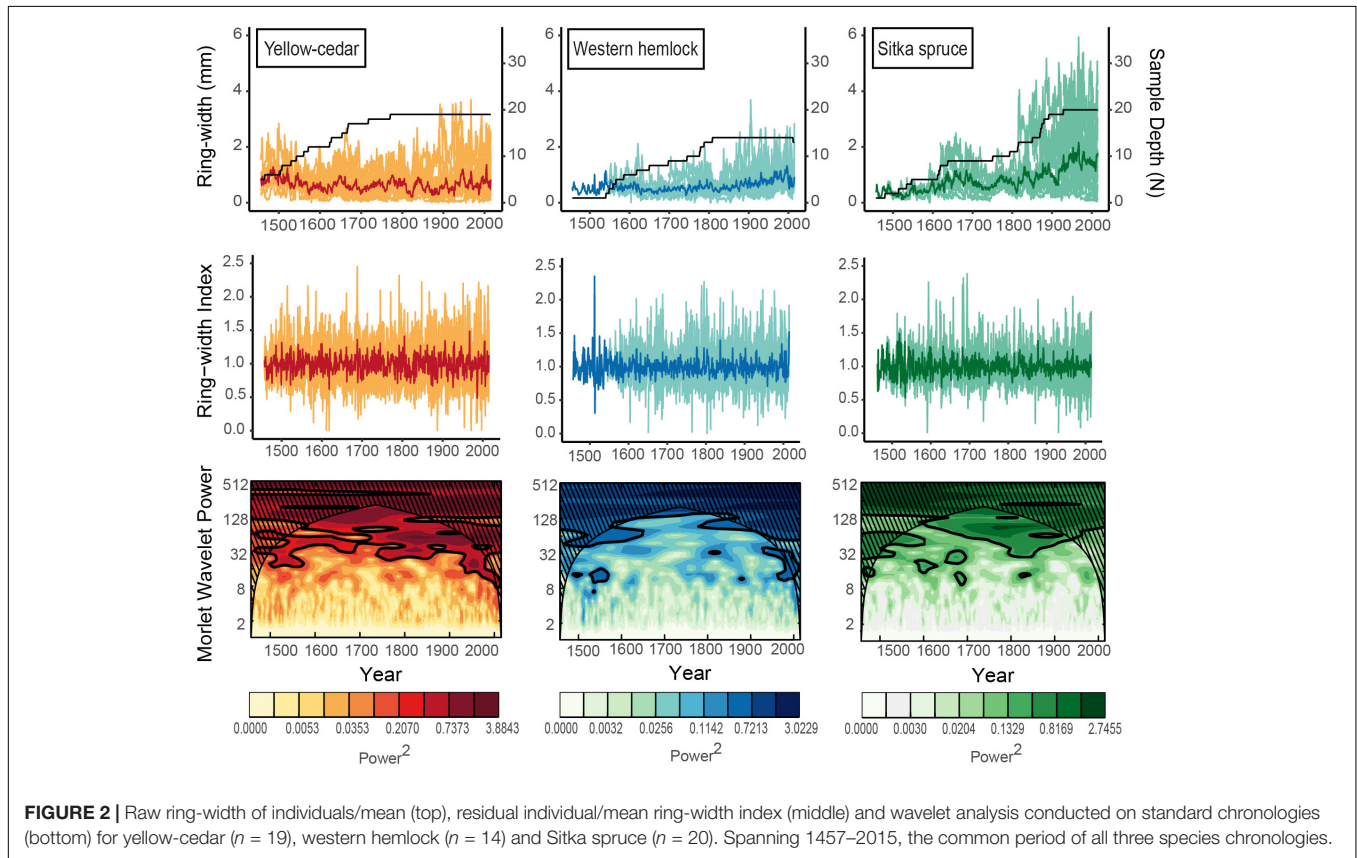

FIGURE 2 | Raw ring-width of individuals/mean (top), residual individual/mean ring-width index (middle) and wavelet analysis conducted on standard chronologies (bottom) for yellow-cedar (*n* = 19), western hemlock (*n* = 14) and Sitka spruce (*n* = 20). Spanning 1457–2015, the common period of all three species chronologies.

(*n* = 14) had the lowest inter-series correlations (rbar = 0.314), while Sitka spruce (*n* = 20) had the lowest inter-annual variability in ring-width (MS = 0.217). Only the yellow-cedar residual chronology exceeded and stayed above a critical EPS value of 0.85, passing the threshold after 1776. Yellow-cedar was also the only species to have an average EPS above 0.85 from 1901 to 2015 (EPS = 0.89).

The chronologies of all three species exhibited inter-annual to multidecadal variation (**Figure 2**). Wavelet analysis highlighted strong multi-decadal variation from 1457 to 2015 that was most stable over time for yellow-cedar and Sitka spruce. Yellow-cedar had strong frequency variation at the 16–128-year wavelengths from 1457 to 2015. Frequency variation at 32–64 years was most stable after 1700. Sitka spruce had strong and stable variation in the 64–128-year wavelengths, and significant variation at 32–64-years around 1800. Western hemlock had the least consistent variation overall, which was significant in the 64–128-year

wavelengths after 1800 and at 16–32-years after 1950, though this interpretation is limited by the weak common signal in the western hemlock chronology.

Climate Comparison Between Time Periods

Annual and monthly maximum temperatures and total precipitation differed significantly among time periods (**Figure 3**). Mean monthly maximum temperatures were consistently cooler from 1946 to 1976 (8.3 ± 5.0°C; mean ± standard deviation) with significant differences in April and June relative to 1901–1945 (8.9 ± 5.1°C) and 1977–2015 (9.0 ± 4.8°C). Temperatures were warmest in May, July, and August during the earliest period (1901–1945) and in January, February, March, and December during the most recent period (1977–2015), although differences were significant
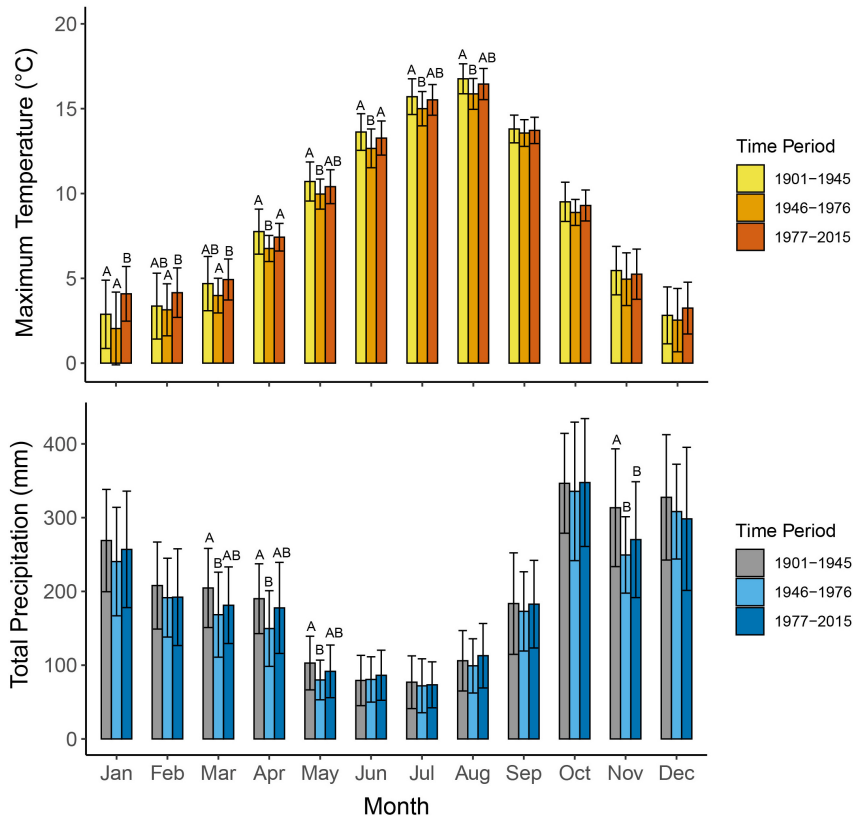
FIGURE 3 | Comparison of monthly maximum temperature and total precipitation between time periods. Each bar represents a monthly temperature or precipitation value averaged across one of the three time periods. Error bars represent standard deviation around the mean. Different letters indicate a significant difference between phases ($p < 0.05$).

in January only. Total annual precipitation was, on average, lower from 1946 to 1976 (2148 ± 242 mm) compared to 1901–1945 (2408 ± 213 mm) and 1977–2015 (2271 ± 311 mm). Precipitation was greatest from 1901 to 1945 for all months except June and August, but significant for November only. Precipitation in June and August was greatest from 1977 to 2015, but not significantly different from other periods.
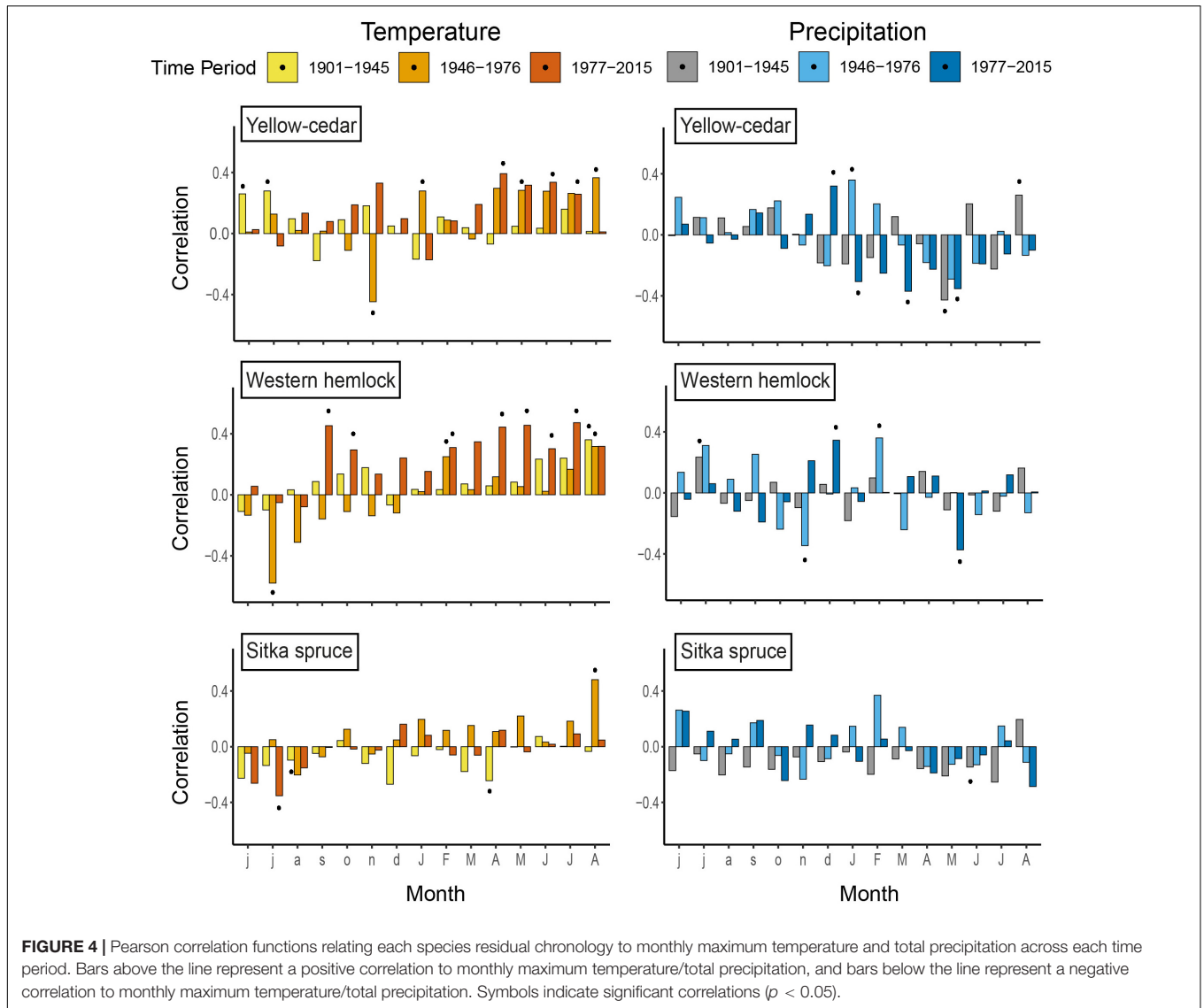
Climate-Growth Correlations With Monthly Climate

Growth of yellow-cedar was positively correlated with maximum temperature but negatively correlated with precipitation during the growing season, with significant but variable relations with winter conditions among time periods (**Figure 4**). From 1901 to 1945 growth was significantly positively correlated to maximum temperature in June and July of the year prior to ring formation, but more strongly correlated to current growing season maximum temperatures after 1946. May precipitation was negatively correlated with growth across all periods, though not significant from 1946 to 1976. Growth was negatively correlated to November temperature and positively correlated to January temperature from 1946 to 1976. Correlations with January temperatures were positive in this period, but negative from 1901

to 1945 and 1977 to 2015, although the negative correlations were not significant. December precipitation had a weak negative correlation with growth prior to 1976, but a significant positive correlation from 1977 to 2015. Correlations with January and February precipitation were positive from 1946 to 1976, negative from 1977 to 2015, and significant for January in both periods.

Western hemlock growth was strongly positively correlated with maximum growing season temperature, with fewer consistent correlations with precipitation (**Figure 4**). From 1901 to 1945, growth was significantly positively correlated to current August temperature and previous July precipitation. From 1946 to 1976, the positive correlation with August temperature persisted but growth was negatively correlated with the previous July temperature. Correlations with precipitation were negative in November but positive in February. The correlations between growth and temperature were strongest in 1977 to 2015, with significant correlations across 7 months spanning the previous fall through current summer. Growth was positively correlated with December precipitation but negatively correlated with May precipitation.

Overall, Sitka spruce growth was weakly correlated to monthly climate across all time periods, with few significant correlations (**Figure 4**). From 1901 to 1945, growth was negatively correlated with previous August and current April temperature and June

FIGURE 4 | Pearson correlation functions relating each species residual chronology to monthly maximum temperature and total precipitation across each time period. Bars above the line represent a positive correlation to monthly maximum temperature/total precipitation, and bars below the line represent a negative correlation to monthly maximum temperature/total precipitation. Symbols indicate significant correlations ($p < 0.05$).

precipitation. Growth was positively correlated with current August temperature from 1946 to 1976 but negatively correlated with previous July temperature from 1977 to 2015.

Growth Response to Growing Season and Winter Climate

The linear-mixed effects models revealed that climate variables affecting growth varied among the species and through time, although with modest explanatory power ($R^2 \leq 0.18$) (**Table 2**). While the predictive effects of some climate variables included in the models were consistent with the correlation analyses, the response of growth to other variables differed, as follows. Yellow-cedar growth was significantly affected by temperature and precipitation across all time periods, with climate explaining the most variation in growth for 1946–1976 ($R^2 = 0.128$) (**Table 2**). November temperature had a positive effect on growth in 1901–1945 and 1977–2015, but a negative effect in 1946–1976.

Winter temperature was significant in all periods, switching from a positive effect in the first two periods, to a negative effect after 1977. Winter precipitation had a negative effect in 1901–1945. In 1901–1945 growth was positively affected by previous summer temperature and August precipitation, but negatively affected by previous September and spring temperature. In 1946–1976, summer temperature positively affected growth, whereas, in 1977–2015 spring temperature positively affected growth.

For western hemlock, all significant predictive effects were during the growing season. In 1901–1945 summer temperature had a positive effect (**Table 2**). Western hemlock was negatively affected by previous summer temperatures in 1946–1976 and 1977–2015, but positively affected by current spring temperatures in both periods. There was a positive effect of previous September temperature in 1977–2015. Climate predicted the greatest variation in western hemlock growth in the most recent time period (1977–2015, $R^2 = 0.173$).

TABLE 2 | Final linear-mixed effects models after model selection, relating tree ring-width index with eight climate variables.

Species	Time period	Intercept	Fixed effects (climate variables)								R^2	RMSE
			$pTMAX_{Sum}$	$pTMAX_{Sept}$	$pTMAX_{Nov}$	$TMAX_{Winter}$	P_{Winter}	$TMAX_{Spring}$	$TMAX_{Sum}$	P_{Aug}		
Yellow-cedar (N = 19)	1901–1945	1.004*** (0.009)	0.059*** (0.009)	−0.034*** (0.010)	0.026** (0.010)	0.022* (0.011)	−0.050*** (0.009)	−0.023* (0.011)		0.028** (0.010)	0.106	0.253
	1946–1976	1.008*** (0.011)			−0.074*** (0.011)	0.024* (0.011)			0.061*** (0.011)		0.128	0.255
	1977–2015	0.999*** (0.011)			0.061*** (0.011)	−0.041*** (0.012)		0.067*** (0.011)			0.081	0.288
Western hemlock (N = 13)	1901–1945	1.003*** (0.010)							0.044*** (0.010)		0.033	0.235
	1946–1976	0.981*** (0.011)	−0.043*** (0.011)					0.024* (0.011)			0.038	0.222
	1977–2015	1.017*** (0.011)	−0.075*** (0.012)	0.081*** (0.012)				0.080*** (0.012)			0.173	0.244
Sitka spruce (N = 17)	1901–1945	0.984*** (0.006)	−0.013* (0.006)							0.013* (0.006)	0.013	0.174
	1946–1976	1.006*** (0.008)					0.022** (0.008)		0.030*** (0.008)		0.038	0.191
	1977–2015	1.006*** (0.007)	−0.021** (0.008)			0.020** (0.008)				−0.022** (0.008)	0.036	0.191

Significance levels = *p < 0.05; **p < 0.01; ***p < 0.001, R^2 = marginal R^2 (variance in growth explained by the climate variables), RMSE = root mean square error. A p before a climate variable indicates the variable was in the previous year. Values in brackets represent the standard error of each coefficient.

Variation in Sitka spruce growth was affected by both winter and growing season conditions, although in all time periods climate predicted limited variation in growth (R^2 = 0.013–0.038) (**Table 2**). Sitka spruce growth was negatively affected by previous summer temperature in 1901–1945 and 1977–2015 but was positively affected by current summer temperature in 1946–1976. August precipitation affected growth positively in 1901–1945 but negatively in 1977–2015. Growth was affected positively by winter precipitation in 1946–1976 and winter temperature in 1977–2015.

DISCUSSION

Climate and Tree Growth Responses Differed Among Pacific Decadal Oscillation Phases

We found that the climate and climate-growth responses of the three co-occurring tree species differed significantly between PDO phases. As hypothesized, we found that maximum monthly temperatures were significantly warmer during positive phases, with the greatest warming in the winter months of the most recent positive phase (1977–2015). Warmer winter temperatures in this most recent period led to an earlier start to the growing season and may have altered the rain-to-snow threshold and underlying hydrology of the forest (Buma et al., 2017). There were a greater number of significant differences in monthly temperature between PDO phases than monthly precipitation, indicating that PDO phase had a greater effect on site temperature than precipitation.

Multi-decadal frequency variation was present in all three species chronologies, suggesting the influence of the PDO. This pattern was strongest for yellow-cedar, less consistent for western hemlock and noticeably absent for Sitka spruce during the twentieth century, suggesting the PDO had a lesser effect on growth variation. Consistent with this, as the climate differed between PDO phases, so too did the strength and direction of climate-growth correlations from which we inferred facilitating and limiting influences of temperature and precipitation on tree growth (Chavardès et al., 2013; Comeau et al., 2019). Both yellow-cedar and western hemlock were strongly facilitated by growing season temperature, while Sitka spruce had weak relations with climate across all phases. We also found that both monthly and seasonal variables could predict variation in species growth among the three phases. The modeled response of residual ring-width index values to growing season and winter climate generally agreed with the correlation analysis, although yellow-cedar responded more strongly to winter temperature. In our models, climate explained only a small proportion of year-to-year variance in ring-width indices for each species, despite the significant correlations of yellow-cedar and western hemlock with climate. Similarly, Campbell et al. (2021) also found low growth variance explained by climate in Pacific coastal forests containing yellow-cedar and western hemlock. The low explanatory power of our chosen climate variables may have been due to the temperate, ocean-moderated climate

or relatively strong influences of local site conditions or gap dynamics inherent to old growth forests. Nevertheless, our study presents novel findings on how the three species growing in the same old-growth forest have responded to climatic variation over the past century and provides insights into how they may respond to future changes in climate if the trees continue to respond in similar ways as they have in the past.

Growing Season Temperatures Facilitate Yellow-Cedar and Western Hemlock Growth

As tree species in high-latitude forests are commonly temperature-limited, we hypothesized that growth would be more positively correlated with and facilitated by temperature during positive phases of the PDO. We found yellow-cedar and western hemlock growth to be strongly facilitated by warmer growing season maximum temperatures, particularly following the transition to a positive PDO phase after 1977. This indicates that growth is being released from a temperature limitation as the regional climate warms, following a similar "greening" response to forests across the circumpolar north (Lloyd and Bunn, 2007). These findings are consistent with positive correlations between temperature and growth of healthy yellow-cedars (Beier et al., 2008; Wiles et al., 2012; Comeau et al., 2019) and western hemlock (Rudnicki and Chen, 2000). The predictive effect of current summer temperature on yellow-cedar and western hemlock growth was less significant than current spring temperatures. Unlike other forests at similar latitudes but in continental climates (Lloyd and Bunn, 2007), climate of our study forest is moderated by the Pacific Ocean and annual rainfall is high. Trees are unlikely to be limited by low soil moisture availability during future growing seasons; therefore, yellow-cedar and western hemlock will likely continue to benefit from warming growing season temperatures.

Sitka spruce exhibited the fastest growth of the three species during the twentieth century, with wide ring widths that were weakly correlated with growing season climate across all PDO phases. Sitka spruce growth was more complacent, with lower mean sensitivity and less multi-decadal variation across the study period than yellow-cedar and western hemlock. The Sitka spruce chronology included the youngest sampled trees, on average, with almost half of the trees younger than 200 years old. Including young, fast growing trees in the chronology could explain the wide average ring-widths in the nineteenth and twentieth century; we found no evidence that the growth rates of older trees increased in response to warming climate. This finding is consistent with research showing that younger, smaller trees are less responsive to climate than older, larger trees (Szeicz and MacDonald, 1994; Carrer and Urbinati, 2004; Trouillier et al., 2019). Sitka spruce growth is limited by low soil moisture during the growing season, low winter temperature (Läänelaid and Helama, 2019) and short growing seasons at upper elevations (Stephen, 1967). In contrast, the mild, wet climate and mid-elevational position of our study site, explains the lack of significant correlations and predictive effects of growing season and winter climate on growth. Considering the weak associations

between climate and growth over the twentieth century, Sitka spruce is least likely to be facilitated or limited by future increases in growing season temperature at our study site on Haida Gwaii.

Relations With Winter Conditions Are an Early Warning of Yellow-Cedar Decline

As hypothesized, yellow-cedar was strongly correlated with and responsive to winter temperature and precipitation during the positive phases of the PDO, as the species is sensitive to warmer winters and snow loss (Hennon et al., 2012; Buma et al., 2017). Contrasting the positive effects of warming growing seasons, yellow-cedar was limited by warm dry winter conditions during the most recent period. This is evidence of the emerging stress to yellow-cedars in recent decades and is consistent with the thaw-freeze hypothesis from Alaska (Hennon et al., 2012). Dividing the time period of analysis based on major switches in the PDO revealed the complex nature of yellow-cedar decline, where the PDO interacts with overarching climate warming. In the earliest time period, spanning the neutral/positive phase, increased radial growth was predicted by warmer drier winter conditions, suggesting yellow-cedar did not benefit from increased moisture over the winter and did not risk thaw-freeze damage with increased winter temperatures. During the cooler negative PDO phase growth was facilitated by warmer wetter January conditions. This follows many other tree species that have exhibited increasing growth over the twentieth century in response to warmer temperatures, leading to longer growing seasons (Driscoll et al., 2005; Wilmking and Juday, 2005; Lloyd et al., 2011), with earlier snowmelt and increased rain-on-snow events (Buma et al., 2017). From 1977 to 2015, when late-winter temperatures were significantly warmer than previous time periods, this relationship switched and growth was limited by low January precipitation and facilitated by higher January precipitation, possibly contributing to a more persistent snowpack insulating yellow-cedars roots from freezing damage. The shallow fine-roots of yellow-cedar rely on a persistent over-winter snowpack for protection from thaw-freeze events (D'Amore and Hennon, 2006; Schaberg et al., 2008). In addition, the models revealed that growth became negatively associated with warmer winter temperature in the 1977–2015 period, which can lead to increased thaw-freeze events as temperatures hover near freezing (Hennon et al., 2012; Buma et al., 2017). This concurs with research from Alaska and Haida Gwaii where warm dry winter conditions have been found to be limiting to yellow-cedar in declining stands (Beier et al., 2008; Wiles et al., 2012; Comeau et al., 2019) and is an early warning sign that these old-growth yellow-cedars are vulnerable to decline.

The negative response of yellow-cedar to warmer winter temperatures from 1977 to 2015 did not appear in the other two species, providing evidence that yellow-cedar is uniquely vulnerable to warming winter climate. Yellow-cedar roots are less cold-tolerant, de-harden earlier, and occupy a shallower soil depth compared to those of western hemlock and Sitka spruce (Schaberg et al., 2005, 2011). However, the relatively high elevation, closed canopy, and well-drained soils of the

forest we studied likely buffered yellow-cedar trees from severe damage by thaw-freeze events in the twentieth century. Snowpack is more persistent and melts later in the spring at high elevations, so the yellow-cedar trees studied growing at mid-elevation (c. 400 masl) on Haida Gwaii were better protected from frost damage than forests closer to sea level (Buma et al., 2017; Comeau et al., 2021), with poorly drained soils (Comeau et al., 2019), where much of the decline on Haida Gwaii has been found.

The sensitivity of yellow-cedar to warm dry winters in recent decades is consistent with other studies showing increased vulnerability to late-winter thaw-freeze events in declining forests (Beier et al., 2008; Comeau et al., 2019, 2021). However, this study is the first to detect this response in an apparently healthy old-growth forest, in which no trees showed visual signs of decline, such as discolored foliage and thinning crowns. When comparing variation in individual ring-width indices from 1900 to 2015, we found some yellow-cedar suffered intermittent growth reductions after 1950 that may be consistent with thaw-freeze events and provide an additional early warning sign of decline (Cailleret et al., 2017; Comeau et al., 2021). We recommend careful monitoring of forest health to determine if canopy dieback or tree mortality of yellow-cedar results in future as winter climate continues to warm.

CONCLUSION

Our research revealed new evidence of yellow-cedar vulnerability to decline, embedded in the rings of trees growing in a seemingly healthy, productive coastal temperate rainforest. Dendrochronology is a valuable tool that can be used to understand how tree growth has responded to past changes in climate. In our novel study, we compared the climate-growth response of three species co-occurring in an old-growth forest on Haida Gwaii. We found Sitka spruce had weak climate-growth responses throughout the twentieth century, with little change in the facilitating and limiting effects of climate following shifts in PDO phase. In contrast, western hemlock and yellow-cedar growth responded strongly to multi-decadal climate variation associated with the PDO and were similarly facilitated by warm growing season temperature after 1946. Yellow-cedar was uniquely limited by warm winter temperatures that reduced snowpacks since 1977, a growth pattern that provides an early warning of species-specific tree susceptibility to decline.

DATA AVAILABILITY STATEMENT

The raw data supporting the conclusions of this article will be made available by the authors, without undue reservation.

AUTHOR CONTRIBUTIONS

LD and VC conceptualized the research, developed, and implemented the field methods. LD, VC, and MC designed the

data analysis and reviewed and edited manuscript drafts. CM conducted formal analyses and interpreted the results. CM and VC prepared draft versions of the manuscript. LD and MC were responsible for project supervision. All authors contributed to the article and approved the submitted version.

REFERENCES

Adams, H. D., Guardiola-Claramonte, M., Barron-Gafford, G. A., Villegas, J. C., Breshears, D. D., Zou, C. B., et al. (2009). Temperature sensitivity of drought-induced tree mortality portends increased regional die-off under global-change-type drought. *Proc. Natl. Acad. Sci. U.S.A.* 106, 7063–7066. doi: 10.1073/pnas.0901438106

Allen, C. D., Macalady, A. K., Chenchouni, H., Bachelet, D., McDowell, N., Vennetier, M., et al. (2010). A global overview of drought and heat-induced tree mortality reveals emerging climate change risks for forests. *For. Ecol. Manag.* 259, 660–684. doi: 10.1016/j.foreco.2009.09.001

BC Government (2020). *Vegetation Resources Inventory – 2020. Data BC.* Available online at: https://data.gov.bc.ca/ (accessed November 3, 2021).

Beier, C. M., Sink, S. E., Hennon, P. E., D'Amore, D. V., and Juday, G. P. (2008). Twentieth-century warming and the dendroclimatology of declining yellow-cedar forests in southeastern Alaska. *Can. J. For. Res.* 38, 1319–1334.

Boisvenue, C., and Running, S. W. (2006). Impacts of climate change on natural forest productivity—evidence since the middle of the 20th century. *Glob. Chang. Biol.* 12, 862–882. doi: 10.1111/j.1365-2486.2006.01134.x

Bourque, C. P. A., Cox, R. M., Allen, D. J., Arp, P. A., and Meng, F. R. (2005). Spatial extent of winter thaw events in eastern North America: historical weather records in relation to yellow birch decline. *Glob. Chang. Biol.* 11, 1477–1492. doi: 10.1111/j.1365-2486.2005.00956.x

Buma, B. (2018). Transitional climate mortality: slower warming may result in increased climate-induced mortality in some systems. *Ecosphere* 9:e02170. doi: 10.1002/ecs2.2170

Buma, B., Batllori, E., Bisbing, S., Holz, A., Saunders, S. C., Bidlack, A. L., et al. (2019). Emergent freeze and fire disturbance dynamics in temperate rainforests. *Austral Ecol.* 44, 812–826. doi: 10.1111/aec.12751

Buma, B., Hennon, P. E., Harrington, C. A., Popkin, J. R., Krapek, J., Lamb, M. S., et al. (2017). Emerging climate-driven disturbance processes: widespread mortality associated with snow-to-rain transitions across 10° of latitude and half the range of a climate-threatened conifer. *Glob. Chang. Biol.* 23, 2903–2914. doi: 10.1111/gcb.13555

Bunn, A., Korpela, M., Biondi, F., Campelo, F., Mérian, P., Qeadan, F., et al. (2021). *DplR: Dendrochronology Program Library in R. R package version 1.7.2.*

Cailleret, M., Jansen, S., Robert, E. M., Desoto, L., Aakala, T., Antos, J. A., et al. (2017). A synthesis of radial growth patterns preceding tree mortality. *Glob. Chang. Biol.* 23, 1675–1690. doi: 10.1111/gcb.13535

Campbell, E. M., Magnussen, S., Antos, J. A., and Parish, R. (2021). Size-, species-, and site-specific tree growth responses to climate variability in old-growth subalpine forests. *Ecosphere* 12:03529. doi: 10.1002/ecs2.3529

Carrer, M., Pellizzari, E., Prendin, A. L., Pividori, M., and Brunetti, M. (2019). Winter precipitation–not summer temperature–is still the main driver for Alpine shrub growth. *Sci. Total Environ.* 682, 171–179. doi: 10.1016/j.scitotenv.2019.05.152

Carrer, M., and Urbinati, C. (2004). Age-dependent tree-ring growth responses to climate in Larix decidua and *Pinus cembra. Ecology* 85, 730–740. doi: 10.1890/02-0478

Cayan, D. R., Kammerdiener, S. A., Dettinger, M. D., Caprio, J. M., and Peterson, D. H. (2001). Changes in the onset of spring in the Western United States. *Bull. Amer. Meteor. Soc.* 82, 399–416.

Chavardès, R. D., Daniels, L. D., Waeber, P. O., Innes, J. L., and Nitschke, C. R. (2013). Unstable climate-growth relations for white spruce in southwest Yukon, Canada. *Clim. Change.* 116, 593–611. doi: 10.1007/s10584-012-0503-8

Christidis, N., Stott, P. A., Brown, S., Karoly, D. J., and Caesar, J. (2007). Human contribution to the lengthening of the growing season during 1950–99. *J. Clim.* 20, 5441–5454. doi: 10.1175/2007JCLI1568.1

Comeau, V. M., Daniels, L. D., Knochenmus, G., Raphaël, D. C., and Zeglen, S. (2019). Tree-rings reveal accelerated yellow-cedar decline with changes to winter climate after 1980. *Forests* 10:1085. doi: 10.3390/F10121085

Comeau, V. M., Daniels, L. D., and Zeglen, S. (2021). Climate-induced yellow-cedar decline on the island archipelago of Haida Gwaii. *Ecosphere* 12:e03427. doi: 10.1002/ecs2.3427

Cook, E. R., and Holmes, R. L. (1996). *Users Manual for Program ARSTAN.* Tucson, AZ: Laboratory of Tree-Ring Research, University of Arizona.

D'Amore, D. V., and Hennon, P. E. (2006). Evaluation of soil saturation, soil chemistry, and early spring soil and air temperatures as risk factors in yellow-cedar decline. *Glob. Chang. Biol.* 12, 524–545.

D'Arrigo, R., Villalba, R., and Wiles, G. (2001). Tree-ring estimates of Pacific decadal climate variability. *Clim. Dyn.* 18, 219–224. doi: 10.1007/s003820100177

D'Arrigo, R., Wilson, R., Liepert, B., and Cherubini, P. (2008). On the 'divergence problem' in Northern Forests: a review of the tree-ring evidence and possible causes. *Glob. Planet. Chang.* 60, 289-305. doi: 10.1016/j.gloplacha.2007.03.004

D'Arrigo, R. D., Kaufmann, R. K., Davi, N., Jacoby, G. C., Laskowski, C., Myneni, R. B., et al. (2004). Thresholds for warming-induced growth decline at elevational tree line in the Yukon Territory, Canada. *Glob. Biogeochem. Cycles* 18:GB3021. doi: 10.1029/2004GB002249

DellaSala, D. A. (2011). *Temperate and Boreal Rainforests of the World: Ecology and Conservation.* Washington, DC: Island Press.

Driscoll, W. W., Wiles, G. C., D'Arrigo, R. D., and Wilmking, M. (2005). Divergent tree growth response to recent climatic warming, Lake Clark National Park and Preserve, Alaska. *Geophys. Res. Lett.* 32:20. doi: 10.1029/2005GL024258

Fritts, H. C. (1976). *Tree Rings and Climate.* London: Academic Press.

Gedalof, Z., and Smith, D. J. (2001). Interdecadal climate variability and regime-scale shifts in Pacific North America. *Geophys. Res. Lett.* 28, 1515–1518. doi: 10.1029/2000GL011779

Groisman, P. Y., Knight, R. W., Karl, T. R., Easterling, D. R., Sun, B., and Lawrimore, J. H. (2004). Contemporary changes of the hydrological cycle over the contiguous United States: trends derived from in situ observations. *J. Hydrometeorol.* 5, 64–85. doi: 10.1175/1525-7541200400<0064:CCOTHC>2.0.CO;2

Harris, A. S. (1990). "Picea sitchensis. (Bong.) Carr. Sitka spruce," in *Silvics of North America, Vol. 1. Agri. Handbook 654*, eds R. M. Burns and B. H. Honkala (Washington, DC: USDA Forest Service), 2260–2267.

Hennon, P. E., D'Amore, D. V., Schaberg, P. G., Wittwer, D. T., and Shanley, C. S. (2012). Shifting climate, altered niche, and a dynamic conservation strategy for yellow-cedar in the North Pacific coastal rainforest. *Bioscience* 62, 147–158. doi: 10.1525/bio.2012.62.2.8

Hennon, P. E., D'Amore, D. V., Zeglen, S., and Grainger, M. (2005). *Yellow-Cedar Decline in the North Coast forest district of British Columbia*. Portland, OR: US Department of Agriculture, Forest Service, Pacific Northwest Research Station, doi: 10.2737/PNW-RN-549

Hennon, P. E., McKenzie, C. M., D'Amore, D. V., Wittwer, D. T., Mulvey, R. L., Lamb, M. S., et al. (2016). *A Climate Adaptation Strategy for Conservation and Management of Yellow-Cedar in Alaska*. Portland, OR: US Department of Agriculture, Forest Service, Pacific Northwest Research Station. doi: 10.2737/PNW-GTR-917

Holliday, J. A., Ritland, K., and Aitken, S. N. (2010). Widespread, ecologically relevant genetic markers developed from association mapping of climate-related traits in Sitka spruce (*Picea sitchensis*). *New Phytol.* 188, 501–514. doi: 10.1111/j.1469-8137.2010.03380.x

Holman, M. L., and Peterson, D. L. (2006). Spatial and temporal variability in forest growth in the Olympic Mountains, Washington: sensitivity to climatic variability. *Can. J. For. Res.* 36, 92–104. doi: 10.1139/x05-225

Holmes, R. L. (1983). Computer-assisted quality control in tree-ring dating and measurement. *Tree Ring Bull.* 43, 69–78. doi: 10.1016/j.dib.2018.08.019

Knowles, N., Dettinger, M. D., and Cayan, D. R. (2006). Trends in snowfall versus rainfall in the Western United States. *J. Clim.* 19, 4545–4559. doi: 10.1175/JCLI3850.1

Kottek, M., Grieser, J., Beck, C., Rudolf, B., and Rubel, F. (2006). World map of the Köppen-Geiger climate classification updated. *Meteorol. Z.* 15, 259-263. doi: 10.1127/0941-2948/2006/0130

Läänelaid, A., and Helama, S. (2019). Climatic determinants of introduced Sitka spruce in Hiiumaa Island, Estonia. *Balt. For.* 25, 161–167. doi: 10.46490/vol25iss1pp161

Laroque, C. P., and Smith, D. J. (1999). Tree-ring analysis of yellow-cedar (*Chamaecyparis nootkatensis*) on Vancouver Island, British Columbia. *Can. J. For. Res.* 29, 115–123. doi: 10.1139/x98-185

Larsson, L. (2014a). *CooRecorder*. Saltsjöbaden: Cybis Elektronik and Data.

Larsson, L. (2014b). *CDendro*. Saltsjöbaden: Cybis Elektronik & Data.

Lertzman, K. P. (1992). Patterns of gap-phase replacement in a subalpine, old-growth forest. *Ecology* 73, 657–669. doi: 10.2307/1940772

Lertzman, K. P. (1995). Forest dynamics, differential mortality and variable recruitment probabilities. *J. Veg. Sci.* 6, 191–204. doi: 10.2307/3236214

Lertzman, K. P., Sutherland, G. D., Inselberg, A., and Saunders, S. C. (1996). Canopy gaps and the landscape mosaic in a coastal temperate rain forest. *Ecology* 77, 1254–1270. doi: 10.2307/2265594

Lévesque, M., Matthias, S., Siegwolf, R., Eilmann, B., Brang, P., Bugmann, H., et al. (2013). Drought response of five conifer species under contrasting water availability suggests high vulnerability of Norway spruce and European larch. *Glob. Chang. Biol.* 19, 3184–3199. doi: 10.1111/gcb.12268

Lloyd, A. H., and Bunn, A. G. (2007). Responses of the circumpolar boreal forest to 20th century climate variability. *Environ. Res. Lett.* 2:045013. doi: 10.1088/1748-9326/2/4/045013

Lloyd, A. H., Bunn, A. G., and Berner, L. (2011). A latitudinal gradient in tree growth response to climate warming in the Siberian taiga. *Glob. Chang. Biol.* 17, 1935-1945. doi: 10.1111/j.1365-2486.2010.02360.x

Mantua, N. J., and Hare, S. R. (2002). The Pacific decadal oscillation. *J. Oceanogr.* 58, 35–44. doi: 10.1023/A:1015820616384

Mantua, N. J., Hare, S. R., Zhang, Y., Wallace, J. M., and Francis, R. C. (1997). A pacific interdecadal climate oscillation with impacts on salmon production. *Bull. Amer. Meteor. Soc.* 78, 1069–1080. doi: 10.1175/1520-04771997078<1069:APICOW>2.0.CO;2

Meidinger, D., and Pojar, J. (1991). *Ecosystems of British Columbia*. Special Report Series 6. Victoria, BC: Ministry of Forests and Range Research Branch.

Meyer, B. F., Buras, A., Rammig, A., and Zang, C. S. (2020). Higher susceptibility of beech to drought in comparison to oak. *Dendrochronologia* 64:125780. doi: 10.1016/j.dendro.2020.125780

Mimura, M., and Aitken, S. N. (2010). Local adaptation at the range peripheries of Sitka spruce. *J. Evol. Biol.* 23, 249–258. doi: 10.1111/j.1420-9101.2009.01910.x

Nakagawa, S., Johnson, P. C. D., and Schielzeth, H. (2017). The coefficient of determination R2 and intra-class correlation coefficient from generalized linear mixed-effects models revisited and expanded. *J. R. Soc. Interface* 14:20170213. doi: 10.1098/rsif.2017.0213

Nemani, R. R., Keeling, C. D., Hashimoto, H., Jolly, W. M., Piper, S. C., Tucker, C. J., et al. (2003). Climate-driven increases in global terrestrial net primary production from 1982 to 1999. *Science* 300, 1560–1563. doi: 10.1126/science.1082750

Packee, E. C. (1990). "*Tsuga heterophylla*," in *Conifers. Silvics of North America*, eds R. M. Burns and B. H. Honkala (Washington, DC: United States Forest Service(USFS), United States Department of Agriculture (USDA), Southern Research Station).

Pinheiro, J., Bates, D., DebRoy, S., Sarkar, D., and R Core Team (2021). *Nlme: Linear and Nonlinear Mixed Effects Models*. Available online at: https://cran.r-project.org/web/packages/nlme/index.html (accessed September 10, 2021).

R Core Team (2021). *R: A Language and Environment for Statistical Computing*. Vienna: R Foundation for Statistical Computing.

Rudnicki, M., and Chen, J. (2000). Relations of climate and radial increment of western hemlock in an old-growth Douglas-fir forest in southern Washington. *Northwest Sci.* 74, 57–68.

Schaberg, P. G., D'Amore, D. V., Hennon, P. E., Halman, J. M., and Hawley, G. J. (2011). Do limited cold tolerance and shallow depth of roots contribute to yellow-cedar decline? *For. Ecol. Manag.* 262, 2142–2150. doi: 10.1016/j.foreco.2011.08.004

Schaberg, P. G., Hennon, P. E., D'amore, D. V., and Hawley, G. J. (2008). Influence of simulated snow cover on the cold tolerance and freezing injury of yellow-cedar seedlings. *Glob. Chang. Biol.* 14, 1282–1293. doi: 10.1111/j.1365-2486.2008.01577.x

Schaberg, P. G., Hennon, P. E., D'Amore, D. V., Hawley, G. J., and Borer, C. H. (2005). Seasonal differences in freezing tolerance of yellow-cedar and western hemlock trees at a site affected by yellow-cedar decline. *Can. J. For. Res.* 35, 2065–2070. doi: 10.1139/x05-131

Shanley, C. S., Pyare, S., Goldstein, M. I., Alaback, P. B., Albert, D. M., Beier, C. M., et al. (2015). Climate change implications in the northern coastal temperate rainforest of North America. *Clim. Change* 130, 155–170. doi: 10.1007/s10584-015-1355-9

Stan, A. B., and Daniels, L. D. (2010). Growth releases of three shade-tolerant species following canopy gap formation in old-growth forests. *J. Veg. Sci.* 21, 74–87. doi: 10.1111/j.1654-1103.2009.01120.x

Stephen, A. F. (1967). *Interpreting the Timberline: An Aid to Help Park Naturalists to Acquaint Visitors with the Subalpine-Alpine Ecotone of Western North America*. San Francisco, CA: U.S. Department of the Interior National Park Service, Western Regional Office, 206.

Stewart, I. T., Cayan, D. R., and Dettinger, M. D. (2004). Changes in snowmelt runoff timing in western North America under a 'business as usual' climate change scenario. *Clim. Chang.* 62, 217–232. doi: 10.1023/B:CLIM.0000013702.22656.e8

Szeicz, J. M., and MacDonald, G. M. (1994). Age-dependent tree-ring growth responses of subarctic white spruce to climate. *Can. J. For. Res.* 24, 120–132. doi: 10.1139/x94-017

Taylor, A. H. (1990). Disturbances and persistence of Sitka Spruce (*Picea sitchensis* (Bong) Carr.) in coastal forests of the Pacific Northwest, North America. *J. Biogeogr.* 17, 47–58. doi: 10.2307/2845187

Torrence, C., and Compo, G. P. (1998). A practical guide to wavelet analysis. *Bull. Amer. Meteor. Soc.* 79, 61–78. doi: 10.1175/1520-04771998079<0061:APGTWA>2.0.CO;2

Trouillier, M., van der Maaten-Theunissen, M., Scharnweber, T., Würth, D., Burger, A., Schnittler, M., et al. (2019). Size matters—a comparison of three methods to assess age-and size-dependent climate sensitivity of trees. *Trees* 33, 183–192. doi: 10.1007/s00468-018-1767-z

Tucker, C. S., and Pearl, J. K. (2021). Coastal tree-ring records for paleoclimate and paleoenvironmental applications in North America. *Quat. Sci. Rev.* 265:107044. doi: 10.1016/j.quascirev.2021.107044

van Mantgem, P. J., Stephenson, N. L., Byrne, J. C., Daniels, L. D., Franklin, J. F., Fulé, P. Z., et al. (2009). Widespread increase of tree

mortality rates in the western United States. *Science* 323, 521–524. doi: 10.1126/science.1165000

Veblen, T. T., Holz, A., Paritsis, J., Raffaele, E., Kitzberger, T., and Blackhall, M. (2011). Adapting to global environmental change in Patagonia: what role for disturbance ecology? *Austral Ecol.* 36, 891–903. doi: 10.1111/j.1442-9993.2010.02236.x

Wang, C. J., Zhang, Z. X., and Wan, J. Z. (2019). Vulnerability of global forest ecoregions to future climate change. *Glob. Ecol. Conserv.* 20:e00760. doi: 10.1016/j.gecco.2019.e00760

Wang, T., Hamann, A., Spittlehouse, D., and Carroll, C. (2016). Locally downscaled and spatially customizable climate data for historical and future periods for North America. *PLoS One* 11:e0156720. doi: 10.1371/journal.pone.0156720

Wigley, T. M., Briffa, K. R., and Jones, P. D. (1984). On the average value of correlated time series with applications in dendroclimatology and hydrometeorology. *J. Appl. Meteor. Climatol.* 23, 201–213. doi: 10.1175/1520-04501984023<0201:OTAVOC<2.0.CO;2

Wiles, G. C., Mennett, C. R., Jarvis, S. K., D'Arrigo, R. D., Wiesenberg, N., and Lawson, D. E. (2012). Tree-ring investigations into changing climatic responses of yellow-cedar, Glacier Bay, Alaska. *Can. J. For. Res.* 42, 814–819. doi: 10.1139/x2012-028

Wilmking, M., and Juday, G. P. (2005). Longitudinal variation of radial growth at Alaska's northern treeline—recent changes and possible scenarios for the 21st century. *Glob. Planet. Change* 47, 282–300. doi: 10.1016/j.gloplacha.2004.10.017

Wilmking, M., Juday, G. P., Barber, V. A., and Zald, H. S. (2004). Recent climate warming forces contrasting growth responses of white spruce at treeline in Alaska through temperature thresholds. *Glob. Chang. Biol.* 10, 1724–1736. doi: 10.1111/j.1365-2486.2004.00826.x

Zang, C., and Biondi, F. (2015). Treeclim: an R package for the numerical calibration of proxy-climate relationships. *Ecography* 38, 431–436. doi: 10.1111/ecog.01335